

High-Resolution Electrochemical Scanning Tunneling Microscopy (EC-STM) Flow-Cell Studies

Marcus D. Lay, Thomas A. Sorenson, and John L. Stickney*

Department of Chemistry, University of Georgia, Athens, Georgia 30602

Received: June 30, 2003

Atomic-level studies involving an electrochemical scanning tunneling microscope (EC-STM) flow-cell are presented. Multiple electrochemical atomic layer epitaxy (EC-ALE) cycles of CdTe formation were observed. For a binary compound (i.e., CdTe), an EC-ALE cycle involves exposure of the substrate to a solution of the first precursor (CdSO₄), followed by exposure to the second precursor (TeO₂), while maintaining potential control. Interleaving blank rinses may also be used, but were omitted in the present studies. To allow the exchange of solutions, the EC-STM cell was modified to allow solution exchange via a single peristaltic pump. A selection valve was used to choose the solution to be introduced into the cell. There is evidence that the growth of the initial layer of CdTe on Au(111), the ($\sqrt{7} \times \sqrt{7}$)-CdTe monolayer, can be improved in homogeneity and morphology by repeatedly depositing and stripping the Cd atomic layer. Therefore, a new starting cycle, which should improve the quality of deposits formed via EC-ALE, has been developed.

Introduction

A number of in-situ techniques, such as surface-enhanced Raman spectroscopy,^{1,2} electrochemical quartz crystal microgravimetry (EQCM),³ and electrochemistry⁴ may provided insights into atomic and molecular scale activities at the solid/liquid interface. However, scanned probe techniques, EC-STM in particular, are unique in their ability to provide an instantaneous real-space atomic level view of the interface.⁵ Hence, there have been ongoing efforts in this group to develop an EC-STM flow-cell. EC-STM studies of the deposition and growth of multiple layers of a compound were needed to provide insight into several areas: the effect of the initial deposition order on deposit structure and morphology; how the surface structure evolves as a function of the number of cycles; the dependence of the deposit structure on the potentials, solution concentrations, identity of the electrolytes, pH, and rinsing.

An EC-STM flow injection system has been previously described.⁶ It was used to investigate the erosion of contaminants on a Au surface after the introduction of an H₂O₂ solution. Morphology changes induced by the H₂O₂ solution, as it flowed into the EC-STM cell, on a large scale (250 × 250 nm) were demonstrated. The present report demonstrates the first use of an EC-STM flow-cell to track surface morphology and atomic layer structure at the atomic scale during multiple solution exchanges, EC-ALE cycles. This article describes the first studies using an EC-STM flow-cell to track the surface morphology and atomic layer structure at the atomic scale during multiple solution exchanges.

Cadmium-chalcogenide II–VI compound thin films, such as CdS, CdSe, CdTe, and HgCdTe, possess a wide range of band gaps and lattice constants, making them a significant set of optoelectronic materials.^{7–9} Though CdTe thin films are generally grown in a vacuum using temperature controlled reactivity, using close spaced vapor deposition methods such as chemical

vapor deposition (CVD)¹⁰ or molecular beam epitaxy (MBE),¹¹ it has also been formed by electrochemical methods.^{12,13}

There are a number of methods for the electrodeposition of compound semiconductors. A method used commercially to form solar cells is referred to as co-deposition. In co-deposition, precursors for both elements in a binary compound are deposited simultaneously at a given potential from a single solution. Co-deposition is advantageous because it is fast and simple and therefore the method of choice in many applications. However, as co-deposition uses a single solution and potential, there are few degrees of freedom for controlling structure, composition, and morphology.

The method of electrochemical atomic layer epitaxy (EC-ALE) has been under development, in this and other groups, for over 10 years. It is the electrochemical analogue of atomic layer epitaxy (ALE), a method based on the alternated deposition of atomic layers of the constituent elements of a compound with atomic level control. ALE can be used with molecular beam epitaxy (MBE) or chemical vapor deposition (CVD) to grow thin films. These methods involve control of the deposit temperature during the alternation of the reactants such that surface limited reactions are used to form each atomic layer.

In electrochemistry, surface limited reactions are referred to as underpotential deposition (upd), a phenomenon by which one element electrodeposits on another at a potential prior to that where the element would deposit on itself.^{14–18} Upd results from the difference in energetics of inter- versus intraelemental bonding; the formation of a surface compound is favorable, as dictated by the accompanying heat of formation. Therefore, upd results in deposition of a single atomic layer. EC-ALE is a combination of upd and ALE. A compound is formed an atomic layer at a time by alternating the solution in contact with the deposit and depositing each element at its upd potential. Thus, one EC-ALE cycle produces one monolayer (ML) of the compound. The number of cycles performed determines the number of ML and the thickness of the deposit. Deposit structure is a function of the crystallography of the deposit and its orientation, as well as the deposition conditions. The deposition

* To whom correspondence should be addressed. E-mail: stickney@sunchem.chem.uga.edu.

process has been automated, allowing micron thick deposits to be formed.^{19,20} An advantage of EC-ALE is that it decomposes compound electrodeposition into a series of steps, which can be thought of as a set of points-of-control. Then, each item can be varied and studied independently.

The electrochemical growth of CdTe on Au(111) has been previously studied via ultrahigh vacuum electrochemistry (UHV-EC) methods such as low energy electron diffraction (LEED) and Auger electron spectroscopy.²¹ Several ordered deposit structures, including a stoichiometric ($\sqrt{7} \times \sqrt{7}$)-CdTe structure with a Cd/Te ratio of 1, were discovered. At higher Cd/Te ratios (1.5 to 2.0) a (3×3)-CdTe structure was observed. From these UHV-EC studies, it was concluded that the ($\sqrt{7} \times \sqrt{7}$)-CdTe and (3×3)-CdTe were the result of forming 1 and 1.5 ML of the compound, respectively, starting with Cd on Au(111) substrates. The highest quality (3×3) LEED images were observed when 1.5 EC-ALE cycles were performed, starting with Cd deposition, though there were signs that similar structures were formed when Te upd was the initial layer.

EC-STM studies of atomic layers of Cd and Te on Au(111) have been reported.^{22–27} Previous studies of the deposition of one cycle of CdTe were achieved by first depositing an initial Te atomic layer on the substrate in an H-cell on the benchtop and then transferring the substrate and atomic layer to the EC-STM cell. The EC-STM cell was then filled with a Cd²⁺ solution, and the formation of a ML of CdTe was imaged. Deposition of Cd upd in an H-cell on the benchtop, followed by transfer to the EC-STM cell was intractable, as the upd Cd layer was unstable at open circuit and spontaneously oxidized upon loss of potential control during the transfer.

This report describes use of a flow-cell for in-situ STM studies of the EC-ALE process. Specifically, to use a cell where the solutions can be exchanged without loss of potential control, so the atomic layers remain stable. Ideally, the structure of each atomic layer will be monitored as it forms. In the present initial study with the flow-cell EC-STM, deposit structure and morphology were monitored through a number of solution exchanges. The conditions chosen were not intended to grow full monolayers of CdTe with each cycle, but simply to allow observation of the deposition process, and surface morphology from step to step.

Experimental Section

The EC-STM flow-cell consisted of a previously described in-situ cell,²⁸ modified to allow solution to flow in near the substrate and out in the reference/auxiliary compartment. The flow rates at the in- and outlet are equivalent, so the volume of solution in the cell is constant. This was accomplished with a single peristaltic pump, flow rate = 0.9 mL/min (Figure 1).

For all experiments, a 99.999% pure Au(111) single crystal (MaTeCK GmbH) was used. The substrate was cleaned in hot nitric acid for 30 min., and then annealed in a hydrogen flame for 7 min. This procedure routinely yielded large atomically flat terraces.

Cd and Te deposition solutions were composed of 0.20 mM CdSO₄ + 1.0 mM H₂SO₄ and 0.25 mM TeO₂ + 10 mM Na₂B₄O₇ + 20 mM Na₂SO₄, respectively. Ultrapure water (>18.1 MΩ) and analytical grade reagents were used. EC-STM studies were carried out in constant current mode (height mode) using a Nanoscope III (Digital Instruments, Santa Barbara, CA). The instrument was previously calibrated by imaging HOPG in air. For all imaging, tips were formed from polycrystalline tungsten wire (diameter = 0.25 mm) etched at 12 V_{AC} in fresh 1 M KOH. To reduce Faradaic currents at the tip/electrolyte

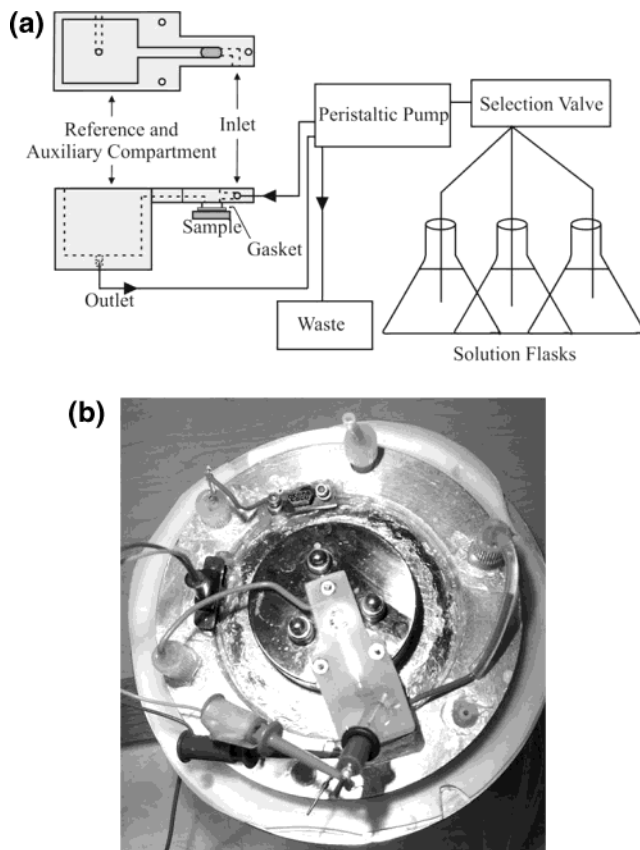


Figure 1. The EC-STM flow-cell: (a) schematic of the EC-STM flow-cell system, (b) image of the EC-STM flow-cell, showing the standard 3-electrode setup, with solution in- and outlet.

interface, tips were coated with hot glue gun glue (Kmart), leaving only the apex exposed. The entire setup, including the cell and scanning head, was isolated from ambient by fitting a Plexiglas hat on top of the microscope, and maintaining a positive pressure of high purity Ar on the system. All potentials were referenced to a 3 M Ag/AgCl reference electrode (BAS), and Au wires served as auxiliary electrodes.

Results and Discussion

The cyclic voltammetry obtained for the Cd and Te solutions used in this study has been previously published.^{20,21,25} Te electrochemistry has a significant pH dependence; the deposition features shift dramatically to more negative potentials as the pH increases, such that the initial Te upd peak occurs at −0.5 V. Consequently, a basic Te solution (pH 9) was used so that atomic layer deposition of both Cd and Te would occur at roughly the same potentials. Problems can arise if a more positive potential is used for deposition of Te than Cd, as after Cd some of the previously deposited Cd may oxidize during Te deposition cycles, given the reversibility of Cd upd.

In the present study, the clean ordered Au(111) crystal was initially placed in the flow-cell, and the Cd solution was introduced. Figure 2 shows a ($4 \times \sqrt{3}$) Cd upd structure on the Au(111) surface at −0.4 V. Similar structures, resulting from the deposition of Cd and adsorbed counterions on Au(111) have been previously observed.^{22,23,25} Coulometry suggested that the Cd coverage was about 0.3 ML, where a ML is one adsorbate species for each surface Au atom. The structure appeared well ordered, and the surface has a smooth morphology. The potential was then shifted to −0.2 V, and the Cd solution was exchanged for the Te. The ($4 \times \sqrt{3}$) structure was still present after the

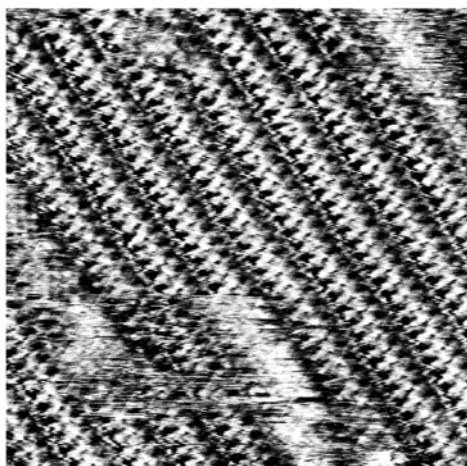


Figure 2. Cd uplayer deposited on Au(111) at -0.40 V vs 3 M Ag/AgCl. Scan size is 10×10 nm.



Figure 3. The Au(111) surface after the deposition of the Cd ($\sqrt{3} \times \sqrt{3}$) and then rinsing in a Te solution. The Te solution was rinsed in at -0.20 V, then the potential was scanned to -0.50 V vs 3 M Ag/AgCl. Scan size is 35×35 nm.

potential change, suggesting the deposited Cd was reasonably stable on the surface at -0.2 V. During the solution exchange, imaging continued, allowing large scale morphology changes to be observed. Atomic resolution was lost during solution exchange however, though Au step-edges were visible.

After introduction of the Te solution, no clear image was observed at -0.2 V. After scanning to -0.5 V, the image shown in Figure 3 was observed. During the negative going scan, a series of atomically high steps, not previously present, were generated as Te deposited. A (3×3) structure appeared to be present on both the upper and lower plateaus, reminiscent of a $4/9$ th coverage (3×3) -Te structure previously reported for Te electrodeposition on Au(111) from acidic electrolyte.²⁶ Evidence of small domains of Cd structures, such as the $(4 \times \sqrt{3})$, were imaged along with the (3×3) -Te. The (3×3) -Te unit cell and the surface roughening (formation of single atom high islands or pits mentioned above) has been previously reported in studies of Te atomic layers on Au(111).²⁹ Ideally, if an atomic layer of Cd was followed by an atomic layer of Te, a monolayer of CdTe would form. Evidently, this not the case in the present study, as most of the surface was covered with Te, with a minority covered by a Cd structure. It may be postulated that the Cd desorbed when the potential was stepped from the initial deposition potential of -0.4 V to -0.2 V, but the micrographs suggest that it was still present after this potential change. The

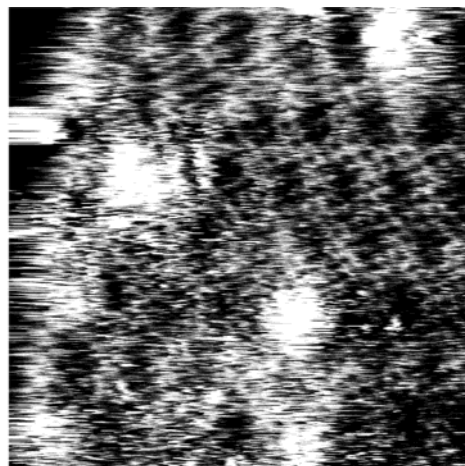


Figure 4. The $(\sqrt{7} \times \sqrt{7})$ -CdTe structure formed after 3 solution changes. Small islands began to nucleate at -0.50 V vs 3 M Ag/AgCl in Cd solution. Scan size is 10×10 nm.

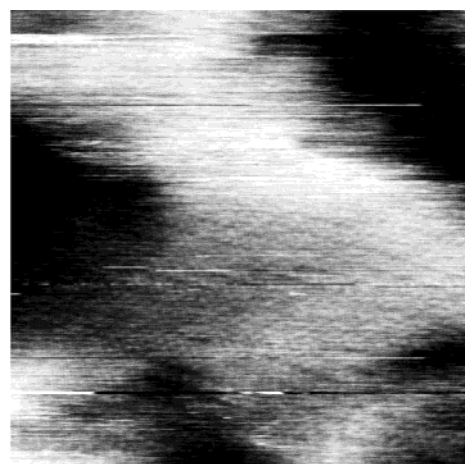


Figure 5. Surface reconstruction observed after the deposition of Te at -0.50 V vs 3 M Ag/AgCl (after 4 solutions changes). Scan size is 15×15 nm.

exchange of the Cd and Te solutions at -0.2 V probably resulted in the loss of most of the Cd from the surface, resulting in the observed loss of order on the surface. Then, as the potential was scanned to -0.5 V, the (3×3) -Te formed, and the remaining Cd was pushed into separate domains. It is interesting to note that the Te did not react with the Cd. This however, is consistent with previous studies where Cd was deposited on a Te coated Au(111) surface.^{21,30} In those studies, Cd upl on Te-coated Au electrodes was shown to be shifted to more negative potentials than on the clean Au surface. The fact that Cd binds more strongly with Au than Te is expected, as Cd is known to form alloys with Au.^{24,25,31,32} So, it is probable that, in the present case, the density of Cd on the surface was not sufficient to promote reaction of the Te with the Cd at least in the potentials used.

The reasons for the roughening transition after formation of the (3×3) -Te are becoming clearer. Work in this group has involved studies of chalcogenide atomic layers formation for the last 10 years, and a roughening transition was repeatedly observed as the coverage of chalcogenide was increased. Most chalcogenides form an initial, low coverage, simple symmetric structure like a $1/3$ coverage $(\sqrt{3} \times \sqrt{3})$.^{33–37} In this structure, the interatomic spacing is larger than the van der Waals diameter.³⁸ When the coverage of the chalcogenide is increased until the inter-chalcogenide distance is less than the van der

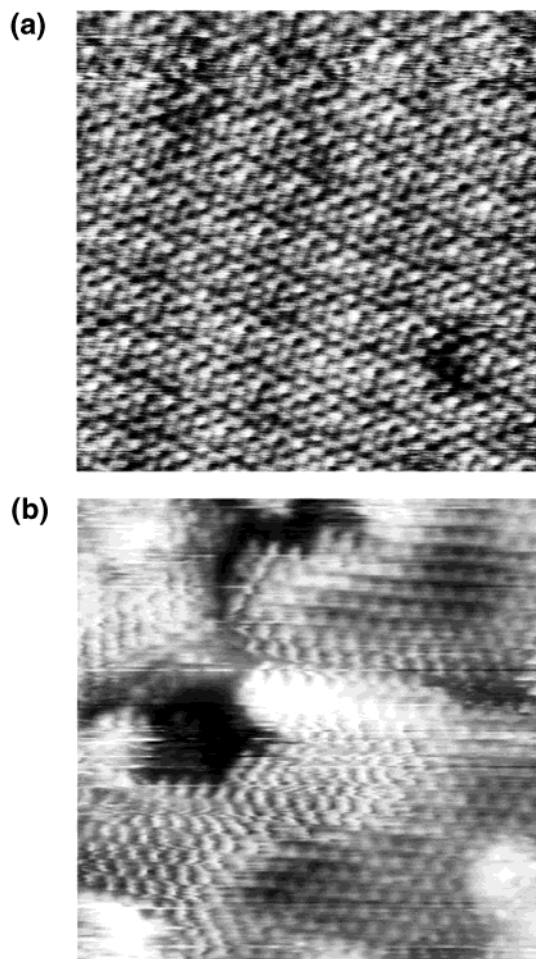


Figure 6. Comparison of the (3×3) -CdTe structures formed: (a) after five solution changes, depositing both elements at -0.5 V vs 3 M Ag/AgCl, (b) after depositing Cd at -0.65 V vs Ag/AgCl on the $(\sqrt{3} \times \sqrt{3})$ -Te with (13×13) domain walls in one step. Scan sizes are 10×10 nm.

Waals diameter, the chalcogenide atoms tend to bond together, forming chains, clusters or rings. Apparently, this process results in surface stress, because the chalcogenides are bound to each other as well as the Au surface, and this stress results in pits or the roughening transition described above; pits similar to those seen in Figure 3, have also been observed for Se deposition on Au(111)³³ and (100),³⁹ S deposition on Au(111)^{40,41} and alkanethiol adsorption on Au(111) surfaces.⁴²

After the next solution exchange of Cd for Te at -0.5 V, the series of plateaus observed after Te deposition disappeared, though there were a number of small islands (Figure 4). The major structure present on the surface involved a $(\sqrt{7} \times \sqrt{7})$ unit cell with a (4×4) moiré pattern. Previous UHV-EC studies have revealed the presences of a $(\sqrt{7} \times \sqrt{7})R19.1^\circ$ structure upon deposition of Cd on Te, or Te on Cd atomic layers, though there was no evidence in the LEED pattern for a (4×4) periodicity.²¹ This previous study suggested that the layer involved a coverage of 3/7th ML of Cd and Te.

It is notable that the surface roughening previously observed was lifted by deposition of the Cd. One possible explanation is that the stress described above, which resulted when the Te atoms began to bind to each other as well as to the Au surface, is relieved when those bonds are broken to form CdTe. The islands visible in Figure 4 have previously been associated with areas of the surface covered with upd Cd. Specifically, as CdTe is a compound semiconductor, tunneling is limited compared to a metallic surface such as Cd upd. There are domains of Cd

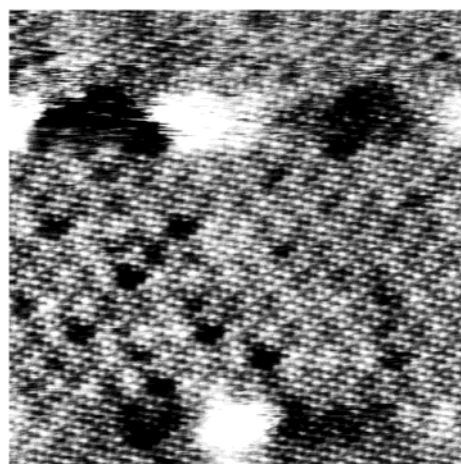


Figure 7. STM micrograph of the (3×3) -Te remaining after oxidizing the Cd from the (3×3) -CdTe at -0.44 V vs 3 M Ag/AgCl. Scan size is 15×15 nm.

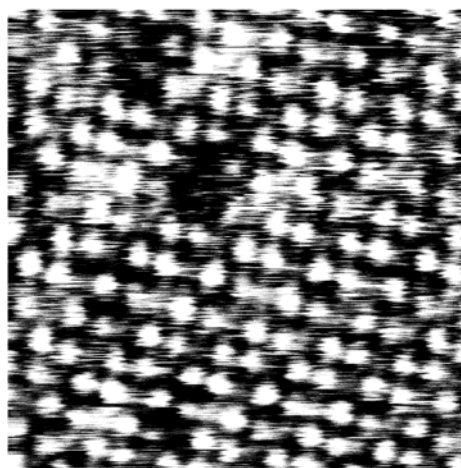


Figure 8. High-resolution STM micrograph of the (3×3) -Te structure, at -0.40 V vs 3 M Ag/AgCl, to contrast it with the (3×3) -CdTe adlayer. The scan size is 5×5 nm.

upd, because prior to the second round of Cd deposition, most of the surface was covered by the (3×3) -Te structure at 4/9th coverage, the coverage needed to form a monolayer of CdTe. However, there were still some domains of Cd upd, so the overall coverage of Te was less than that needed to form a full monolayer of CdTe. When Cd was deposited on this surface, CdTe did not cover the entire surface, thus Cd upd was present.

A fourth solution change, from Cd back again to Te, was performed at -0.50 V. Surprisingly, the Cd was again stripped from the surface upon introduction of the Te solution as the (3×3) -Te structure was evident, and the surface roughened, as would be expected if the Cd atoms were removed from the surface (Figure 5). One point to be considered is that the Te deposition solution was pH 9. This pH shifts the stripping potential for Cd considerably more negative than when deposited from the pH 3 Cd solutions.

Subsequent introduction of the Cd solution to the electrochemical cell, this time at -0.54 V resulted in the adlayer in Figure 6a. Again, the surface shows the $(\sqrt{7} \times \sqrt{7})$ -CdTe monolayer. The deposit appears surprisingly smooth, as if each time the Cd is deposited and then removed, the monolayer improved in quality. In a separate experiment, designed to facilitate comparison, Cd was deposited at more cathodic potentials in a single step (no solution exchanges). These

conditions led to a decrease in grain size, and the formation of a $(\sqrt{3} \times \sqrt{3})$ -CdTe structure (Figure 6b).

After the formation of the $(\sqrt{7} \times \sqrt{7})$ -CdTe structure in 5 solution changes, the potential was stepped positively to -0.44 V. At this potential, Cd was oxidized from the deposit, leaving only Te atoms on the electrode. After this process, the 4/9th coverage (3×3) -Te was observed (Figure 7). Some pits were also observed. Figure 8 shows a close-up of the (3×3) -Te, to facilitate comparison with the (3×3) -CdTe.

It must be noted that in the formation of CdTe thin films using EC-ALE, the potential program described here has not been used. As is evident, this program results in the deposition of Cd on the Au substrate or a Te adlayer, and then its subsequent stripping. A single monolayer, the $(\sqrt{7} \times \sqrt{7})$ -CdTe structure, is the most CdTe that is formed. It appears, however, that each time the Cd is dissolved in the basic Te solution, a little more Te is deposited, and then when the Cd is re-deposited, a smoother, more crystalline CdTe deposit is formed.

To sequentially build up a thin film of CdTe using layer by layer growth, these initial potentials would need to be shifted more negatively after the first few cycles, as has been described previously.²⁰ The program presented herein was intended to be an EC-STM investigation of the chemistry that occurs during initial cycles during EC-ALE.

Conclusions

An EC-STM flow-cell has been used for in-situ atomic-level observations of the first monolayer of CdTe growth on a Au-(111) surface. Solution exchange was performed during the imaging process. Deposition of Te led to a surface roughening, which was alleviated during subsequent Cd deposition. The first monolayer of CdTe appears to have a $(\sqrt{7} \times \sqrt{7})$ structure, as previously observed with LEED. When the $(\sqrt{7} \times \sqrt{7})$ -CdTe was formed in the first cycle, the morphology appeared rough. However, when this $(\sqrt{7} \times \sqrt{7})$ -CdTe monolayer was formed by repeatedly depositing and stripping Cd on the Te adlayer, the initial rough monolayer became much smoother, suggesting a better way of initiating thin film deposition. Therefore, the quality of the first monolayer of the compound on the Au substrate, the $(\sqrt{7} \times \sqrt{7})$ -CdTe, may be manipulated using a cycle wherein the Cd is deposited and stripped several times, before the program proceeds with deposition of a thin film. This can produce a well ordered first monolayer (Figure 6a), on which to build subsequent deposits. Alternatively, direct deposition of the first monolayer can result in a fairly disordered structure, such as that shown in Figure 6b. Such disorder in the first monolayer suggests that subsequent deposition will have an increased degree of disorder as well.

References and Notes

- (1) Zou, S.; Weaver, M. J. *Chem. Phys. Lett.* **1999**, *312*, 101.
- (2) Marenco, C.; Stirling, C. J. M.; Yarwood, J. J. *Raman Spectrosc.* **2001**, *32*, 183.
- (3) Tsionsky, V.; Gileadi, E. *Mat. Sci. Eng., A* **2001**, *302*, 120.
- (4) Bard, A. J.; Faulkner, L. R. *Electrochemical Methods, Fundamentals, and Applications*, 1st ed.; John Wiley & Sons: New York, 1980.
- (5) Gewirth, A. A.; Niece, B. K. *Chem. Rev.* **1997**, *97*, 1129.
- (6) Noll, J. D.; Vanpatten, P. G.; Nicholson, M. A.; Booksh, K.; Myrick, M. L. *Rev. Sci. Instrum.* **1995**, *66*, 4150.
- (7) Gore, R. B.; Pandey, R. K.; Kulkarni, S. K. *J. Appl. Phys.* **1989**, *65*, 2693.
- (8) Loizos, Z.; Mitsis, A.; Spyrellis, N.; Froment, M.; Maurin, G. *Thin Solid Films* **1993**, *235*, 51.
- (9) Ozaki, T.; Iwase, Y.; Takamura, H.; Ohmori, M. *Nucl. Instrum. Methods Phys. Res., Sect. A* **1996**, *380*, 141.
- (10) Berrigan, R. A.; Maung, N.; Irvine, S. J. C.; Cole-Hamilton, D. J.; Ellis, D. J. *Cryst. Growth* **1998**, *195*, 718.
- (11) Compaan, A.; Bhat, A.; Tabory, C.; Liu, S.; Nguyen, M.; Aydinli, A.; Tsien, L. H.; Bohn, R. G. *Sol. Cells* **1991**, *30*, 79.
- (12) Danaher, W. J.; Lyons, L. E. *Nature* **1978**, *271*, 139.
- (13) Panicker, M. P. R.; Knaster, M.; Kroger, F. A. *J. Electrochem. Soc.* **1978**, *125*, 566.
- (14) Kolb, D. M. Physical and Electrochemical Properties of Metal Monolayers on Metallic Substrates. In *Advances in Electrochemistry and Electrochemical Engineering*; Gerischer, H., Tobias, C. W., Eds.; John Wiley: New York, 1978; Vol. 11; p 125.
- (15) Juttner, K.; Lorenz, W. J. Z. *Phys. Chem. N. F.* **1980**, *122*, 163.
- (16) Adzic, R. R. Electrocatalytic Properties of the Surfaces Modified by Foreign Metal Ad Atoms. In *Advances in Electrochemistry and Electrochemical Engineering*; Gerischer, H. and Tobias, C. W., Eds. Wiley-Interscience: New York, 1984; Vol. 13; p 159.
- (17) Gewirth, A. A.; Niece, B. K. *Chem. Rev.* **1997**, *97*, 1129.
- (18) Herrero, E.; Buller, L. J.; Abruna, H. D. *Chem. Rev.* **2001**, *101*, 1897.
- (19) Wade, T. L.; Ward, L. C.; Maddox, C. B.; Happek, U.; Stickney, J. L. *Electrochem. Solid-State Lett.* **1999**, *2*, 616.
- (20) Flowers, B. H.; Wade, T. L.; Garvey, J. W.; Lay, M.; Happek, U.; Stickney, J. L. *J. Electroanal. Chem.* **2002**, *524*, 273.
- (21) Varazo, K.; Lay, M. D.; Sorenson, T. A.; Stickney, J. L. *J. Electroanal. Chem.* **2002**, *522*, 104.
- (22) Hsieh, S. J.; Gewirth, A. A. *Langmuir* **2000**, *16*, 9501.
- (23) Bondos, J. C.; Gewirth, A. A.; Nuzzo, R. G. *J. Phys. Chem.* **1996**, *100*, 8617.
- (24) Lay, M. D.; Stickney, J. L. *J. Am. Chem. Soc.* **2003**, *125*, 1352.
- (25) Lay, M. D.; Varazo, K.; Srisook, N.; Stickney, J. L. *J. Electroanal. Chem.* **2003**, in press.
- (26) Sorenson, T. A.; Varazo, K.; Suggs, D. W.; Stickney, J. L. *Surf. Sci.* **2001**, *470*, 197.
- (27) Sorenson, T. A.; Lister, T. E.; Huang, B. M.; Stickney, J. L. *J. the Electrochem. Soc.* **1999**, *146*, 1019.
- (28) Suggs, D. W.; Bard, A. J. *J. Am. Chem. Soc.* **1994**, *116*, 10725.
- (29) Sorenson, T. A.; Varazo, K.; Suggs, D. W.; Stickney, J. L. *Surf. Sci.* **2001**, *470*, 197.
- (30) Suggs, D. W.; Stickney, J. L. *Surface Science* **1993**, *290*, 362.
- (31) Takamura, T.; Takamura, K.; Nippe, W.; Yeagar, E. *J. Electrochem. Soc.* **1970**, *117*, 626.
- (32) Astley, D. J.; Harrison, J. A.; Thirsk, H. R. *J. Electroanal. Chem.* **1968**, *19*, 325.
- (33) Lister, T. E.; Stickney, J. L. *J. Phys. Chem.* **1996**, *100*, 19568.
- (34) Andreasen, G.; Vericat, C.; Vela, M. E.; Salvarezza, R. C. *J. Chem. Phys.* **1999**, *111*, 9457.
- (35) Vericat, C.; Andreasen, G.; Vela, M. E.; Salvarezza, R. C. *J. Physical Chem. B* **2000**, *104*, 302.
- (36) Martin, H.; Vericat, C.; Andreasen, G.; Creus, A. H.; Vela, M. E.; Salvarezza, R. C. *Langmuir* **2001**, *17*, 2334.
- (37) Gao, X. P.; Zhang, Y.; Weaver, M. J. *J. Phys. Chem.* **1992**, *96*, 4156.
- (38) Pauling, L. *The Nature of the Chemical Bond*, 3rd ed.; Cornell University Press: Ithaca, NY, 1960.
- (39) Huang, B. M.; Lister, T. E.; Stickney, J. L. *Surf. Sci.* **1997**, *392*, 27.
- (40) Gao, X.; Zhang, Y.; Weaver, M. J. *J. Phys. Chem.* **1992**, *96*, 4156.
- (41) McCauley, R. L.; Kim, Y. T.; Bard, A. J. *J. Phys. Chem.* **1993**, *97*, 211.
- (42) Touzov, I.; Gorman, C. B. *J. Phys. Chem. B* **1997**, *101*, 5263.